CRYSTAL GROWTH & DESIGN



Article

# Fluorinated Aminopyridines: Synthesis, Structure, and Rare Liquid-Liquid Cocrystal Formation Driven by Unusually Short N–H···F–C Hydrogen Bonding

Andrew J. Peloquin, Daniel A Kure, Abby R Jennings, Colin D. McMillen, Scott T Iacono, and William T. Pennington

*Cryst. Growth Des.*, **Just Accepted Manuscript** • DOI: 10.1021/acs.cgd.0c00689 • Publication Date (Web): 16 Jun 2020

# Fluorinated Aminopyridines: Synthesis, Structure, and Rare Liquid-Liquid Cocrystal Formation Driven by Unusually Short N–H···F–C Hydrogen Bonding

*Andrew J. Peloquin,† Daniel A. Kure,‡ Abby R. Jennings,‡ Colin D. McMillen,*

*Scott T. Iacono,*,‡ and William T. Pennington*,†*

†Department of Chemistry, Clemson University, 219 Hunter Laboratories, Clemson, SC 29634

‡ Department of Chemistry & Chemistry Research Center, Laboratories for Advanced Materials, United States Air Force Academy, 2355 Fairchild Dr, Suite 2N-225, Colorado Springs, CO 80840

perfluoropyridine, crystal engineering, fluorine, hydrogen bonds, non-covalent interactions

**Abstract:** The role of hydrogen bonding in the crystal packing of a series of 4-aminoperfluoropyridines was studied using single-crystal X-ray crystallography. The aminoperfluoropyridines were synthesized using only excess amine to serve as both nucleophile and base. Instead of addition to the perfluoropyridine ring, a strong N–H•••F–C hydrogen bond led to co-crystal formation of perfluoropyridine with sterically hindered amines dicyclohexylamine as well as 2-methylpiperdine. This formation is, to our knowledge, the first report of two non-reacting liquids, consisting of only discrete small molecules, combining to form a cocrystalline solid stable under ambient conditions. Perfluoropyridine is stabilized in the crystal lattice approximately 100 °C above its normal boiling point.

## INTRODUCTION

Despite its increasing synthetic utility and prevalence in bio-active molecules, the ability of organic fluorine to participate in hydrogen bonding is a debated topic, particularly when referring to C–H•••F–C interactions and their role in crystal engineering. When a stronger hydrogen bond donor is present, such as N–H or O–H,

there is some consensus that the interaction with organic fluorine is an attractive force, but it is considerably weaker than interactions with more common acceptors.[1–5]

One major source of evidence of the prevalence of interactions with organic fluorine comes from single-crystal X-ray crystallography. Several surveys of the Cambridge Structural Database (CSD)[6] specifically focused on C–F•••H interactions have been published over the last decades.[7–14] In each case, the authors acknowledge that while *X*–H•••F–C hydrogen bonds do occur, they are rare relative to more traditional hydrogen bonding interactions to oxygen and nitrogen. One particular study attributes the majority of these contacts as occurring either from the lack of stronger acceptors, or a high fluorine content, or that the contact is incidental, such as in a bifurcated hydrogen bond. The authors conclude the *X*–H•••F–C hydrogen bond is uncompetitive in nature and is "a donor's last resort."[15]

To study these unusual and non-preferred influences of the C–F bonds in crystal packing, a substrate pool was developed containing a variety of groups capable of hydrogen bonding. A recent computational study of the addition of the phenoxide ion to perfluoropyridine (**1**) indicated an uneven electron distribution across the fluorine

positions, with an increase in electron density in the *para* fluorine of this ring system relative to the other fluorine positions, making it a preferred entity to act as a *X*–H•••F hydrogen bond acceptor.[16] (Scheme 1) Perfluoropyridine is commercially available and inexpensive, while undergoing highly selective and well understood substitution chemistry. Numerous methods to accomplish the substitution have been reported, making it an ideal candidate for this study. More complex synthetic approaches are often employed, including the most common method involving the use of a carbonate or alkoxide base in a solvent of acetonitrile or dimethylformamide.[17–19] Amine bases have also been successfully utilized.[20–24] 4-amino substituted perfluoropyridines have also been accessed by copper catalysed coupling of 2,3,5,6-tetrafluoropyridine and *O*-benzoylhydroxyamines.[25]

**Scheme 1.** Addition or hydrogen bonding with perfluoropyridine

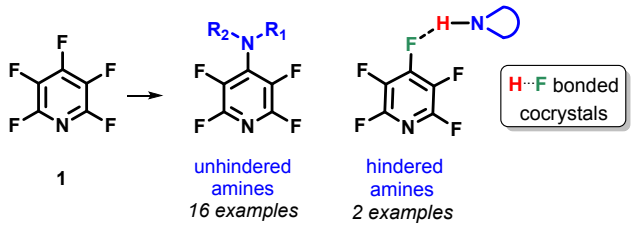


## EXPERIMENTAL SECTION

**Materials.** All solvents and reagents were commercially available and used as received. Bulk solvents were purchased from Pharmco-Aaper. Deuterated solvents were purchased from Cambridge Isotopes Laboratories. Pentafluoropyridine was purchased from SynQuest Laboratories. All other reagents were purchased from Oakwood Chemical.

**Physical Measurements.** $^{1}H$, $^{13}C$, and $^{19}F$ NMR data were obtained the JOEL JNM-ECZ500R/S1 NMR at probe temperature using commercially available deuterated solvents. All chemical shifts (*s* = singlet; *d* = doublet; *t* = triplet; *m* = multiplet, *dd* = doublet of doublets, *dt* = doublet of triplets) are reported in parts per million (ppm). $^{1}H$ chemical shifts were referenced to residual protio-solvent.[26] Melting points were determined via differential scanning calorimetry on a TA Q200 DSC utilizing aluminum pans. The analyses were carried out using a 5 °C/min temperature gradient under nitrogen. Elemental analyses were performed with a Thermo Elementar Vario EL III combustion analyzer using sulfanilamide as a standard. The combustion and reduction tubes were held at 1150 and 950 °C, respectively, under a stream of argon carrier gas at 1100–1200 mbar pressure.

**X-ray Crystallography.** For single-crystal x-ray analysis, crystals were mounted on low background cryogenic loops using paratone oil. Data were collected using Mo Kα radiation (λ = 0.71073 Å) on a Bruker D8 Venture diffractometer with a Incoatec Iμs microfocus source and a Photon 2 detector, a Bruker D8 Quest diffractometer with a Photon 100 detector, or a Bruker SMART APEX CCD diffractometer. Diffraction data were collected using φ and ω-scans and subsequently processed (SAINT) and scaled (SADABS) using the APEX3 software suite.[27] The structures were solved by intrinsic phasing (SHELXT) and refined by full-matrix least square techniques (SHELXL) on $F^2$ using the SHELXTL software suite.[28] All nonhydrogen atoms were refined anisotropically. All OH and NH hydrogen atoms were refined with appropriate DFIX restraints, while all other hydrogen atoms were placed in geometrically optimized positions using the appropriate riding models. Crystallographic data from the structure refinements is provided in the Supporting Information.

Powder x-ray diffraction measurements were completed by the Bragg–Brentano focusing method on a Rigaku Ultima IV X-ray diffractometer with a CuKα radiation source and a CuKβ filter at an operating voltage and current of 40 kV and 40 mA,

respectively. Measurement profiles were collected from 5° to 65° in continuous scan mode at 1 deg $min^{-1}$ with a step width of 0.01° on a $\theta/2\theta$ scan axis.

Electrostatic potentials were mapped onto the Hirshfeld Surface using CrystalExplorer.[29,30] Wavefunctions were calculated at B3LYP/6-31G(d,p) level. In all figures, the molecular ESP is mapped on surfaces over the range -0.05 au (red), through zero (white), to 0.05 au (blue); 1 au = 2625.5 kJ mol-1 per unit charge.

**Synthesis of 4-amino-2,3,5,6-tetrafluoropyridines.** Synthesis of compounds **2**, **3**, **5**, **8**, and **10–12** have been previously reported in the literature by varying methods and yielded reproducible NMR spectra.[20,25,31,32]

*$N^1$, $N^2$-bis(perfluoropyridine-4-yl)ethane-1,2-diamine (2).* To a solution of perfluoropyridine (1 mL, 9.11 mmol) in EtOH (5 mL) maintained at 0 °C, ethylenediamine (0.66 mL, 10.0 mmol) in EtOH (2 mL) was added. The white precipitate was collected after 5 mins (1.32 g, 81%). Crystals suitable for single-crystal x-ray diffraction were obtained by slow evaporation of an ethyl acetate solution of the compound.

*N*[1], *N*[3]*-bis(perfluoropyridine-4-yl)propane-1,3-diamine (3).* Compound **3** was synthesized according to the same procedure as **2** utilizing propanediamine (0.84 mL, 10.0 mmol). The white precipitate was collected after 5 mins (1.42 g, 84%). Crystals suitable for single-crystal x-ray diffraction were obtained by dissolving the product in refluxing EtOH, then cooling to room temperature.

*N*[1], *N*[6]*-bis(perfluoropyridine-4-yl)hexane-1,6-diamine (4).* Compound **4** was synthesized according to the same procedure as **2** utilizing hexamethylenediamine (1.39 mL, 10.0 mmol). The white precipitate was collected after 5 mins (1.43 g, 76%). Crystals suitable for single-crystal x-ray diffraction were obtained by dissolving the product in refluxing EtOH, then cooling to room temperature. Mp 114 °C. $^{1}$H NMR ($CDCl_3$, 500 MHz): δ 4.57 (2H, *s*, N*H*), 3.53 (4H, *t*, $^{3}J_{HH}$ = 6.0 Hz, NHC$H_2$CH$_2$CH$_2$), 1.66, (4H – overlapping with $H_2O$, *br s*, NHCH$_2$CH$_2$C$H_2$), 1.44 (4H, *m*, NHCH$_2$C$H_2$CH$_2$). $^{13}$C{$^{1}$H} NMR ($CDCl_3$, 126 MHz): δ 145.6–143.0 (*m*), 138.0–137.5 (*m*), 132.4–130.0 (*m*), 44.9 (NH*C*H$_2$CH$_2$CH$_2$), 30.8 (NHCH$_2$*C*H$_2$CH$_2$), 26.3 (NHCH$_2$CH$_2$*C*H$_2$). $^{19}$F NMR ($CDCl_3$, 471 MHz): δ -94.2 (4F, NC*F*CFC), -164.4 (4F, NCFC*F*C). Anal Calcd for $C_{16}H_{14}F_8N_4$ (414.11): C, 46.39; H, 3.41; N, 13.52; Found: C, 46.03; H, 3.38; N, 13.86.

*$N^1$-(perfluoropyridin-4-yl)-$N^2$-(2-((perfluoropyridin-4-yl)amino)ethyl)ethane-1,2-diamine (**5**).* Compound **5** was synthesized according to the same procedure as **2** utilizing diethylenetriamine (1.08 mL, 10.0 mmol). The white precipitate was collected after 5 mins (1.67 g, 92%). Crystals suitable for single-crystal x-ray diffraction were obtained by dissolving the product in refluxing EtOH, then cooling to room temperature.

*2,3,5,6-tetrafluoro-N-(1-phenylethyl)pyridin-4-amine (**7**).* Compound **7** was synthesized according to the same procedure as **2** utilizing α-methylbenzylamine (2.58 mL, 20.0 mmol). After 48 hours, the reaction mixture was decanted and the colorless solid triturated with cold EtOH (3 x 10 mL). Upon warming to room temperature and removal of residual solvent *in vacuo*, the product was obtained as a colorless oil (1.72 g, 70%). $^1$H NMR ($CDCl_3$, 500 MHz): δ 7.37–7.30 (5H, *m*, NHCH($CH_3$)*Ph*), 5.11 (1H, *d*, $^3J_{HH}$ = 6 Hz, NHC*H*($CH_3$)Ph), 4.85 (1H, *br s*, N*H*CH($CH_3$)Ph), 1.62, (3H, *d*, $^3J_{HH}$ = 6 Hz, NHCH(C*H*$_3$)Ph). $^{13}$C{$^1$H} NMR ($CDCl_3$, 126 MHz): δ 145.4–143.2 (*m*), 143.4 (NHCH($CH_3$)*Ph*), 137.0-136.6 (*m*), 132.5–130.0 (*m*), 129.1 (NHCH(CH3)*Ph*), 127.9 (NHCH($CH_3$)*Ph*), 125.6 (NHCH($CH_3$)*Ph*), 54.3 (NH*C*H($CH_3$)Ph), 24.6 (NHCH(*C*$H_3$)Ph). $^{19}$F NMR ($CDCl_3$, 471 MHz): δ -93.8 (2F, NC*F*CFC), -162.5 (2F, NCFC*F*C). Anal Calcd

for $C_{13}H_{10}F_4N_2$ (270.08): C, 57.78; H, 3.73; N, 10.37; Found: C, 57.75; H, 3.78; N, 10.76.

*2,3,5,6-tetrafluoro-4-(pyrrolidin-1-yl)pyridine (**8**).* Compound **8** was synthesized according to the same procedure as **2** utilizing pyrrolidine (1.65 mL, 20.0 mmol). The white precipitate was collected after 12 hrs (1.56 g, 78%). Crystals suitable for single-crystal x-ray diffraction were obtained by dissolving the product in refluxing EtOH, then cooling to room temperature.

*4-(2,5-dihydropyrrol-1-yl)-2,3,5,6-tetrafluoropyridine (**9**).* Compound **9** was synthesized according to the same procedure as **2** utilizing 3-pyrroline (1.52 mL, 20.0 mmol). The white precipitate was collected after 12 hrs (1.75 g, 88%). Crystals suitable for single-crystal x-ray diffraction were obtained by diffusion of EtOH into an ethylacetate solution. Mp 122 °C. $^1$H NMR ($CDCl_3$, 500 MHz): δ 5.88 (2H, *s*, $NHCH_2CH$), 4.66 (4H, *t*, $^3J_{HH}$ = 3.5 Hz, $NHCH_2CH$). $^{13}$C{$^1$H} NMR ($CDCl_3$, 126 MHz): δ 146.8–144.7 (*m*), 137.0–136.6 (*m*), 132.7–130.4 (*m*), 125.1 ($NHCH_2CH$), 58.2 (*t*, $^4J_{CF}$ = 7.3 Hz, $NHCH_2CH$). $^{19}$F NMR ($CDCl_3$, 471 MHz): δ -94.9 (2F, $NCFCFC$), -161.9 (2F, $NCFCFC$). Anal Calcd for $C_9H_6F_4N_2$ (218.05): C, 49.55; H, 2.77; N, 12.84; Found: C, 49.42; H, 2.86; N, 13.02.

*2,3,5,6-tetrafluoro-N-phenylpyridin-4-amine (**11**).* Compound **11** was synthesized according to the same procedure as **2** utilizing aniline (1.83 mL, 20.0 mmol). The product was collected as colorless crystals after 12 hrs (1.82 g, 82%). Crystalline product collected by this method was of sufficient quality for single-crystal x-ray diffraction.

*$N^1$-(perfluoropyridin-4-yl)benzene-1,4-diamine (**12**).* Compound **12** was synthesized according to the same procedure as **2** utilizing 1,4-phenylenediamine (2.17 g, 20.0 mmol) dissolved in THF (2 mL). The product was collected as off-white crystals after 30 mins (2.21 g, 94%). Mp 191 °C. $^1$H NMR (DMSO-$d_6$, 500 MHz): δ 9.00 (1H, *s*, N*H*ArNH2), 6.89 (2H, *d*, $^3J_{HH}$ = 10.5 Hz, NH*Ar*$NH_2$), 6.54 (2H, *d*, $^3J_{HH}$ = 7.0 Hz, NH*Ar*$NH_2$), 5.05 (2H, *s*, NHArN*$H_2$*). $^{13}$C{$^1$H} NMR ($CDCl_3$, 126 MHz): δ 146.7 (NH*Ar*$NH_2$), 145.0–142.6 (*m*), 136.6–136.6 (m), 132.6–130.2 (*m*), 127.6 (NH*Ar*$NH_2$), 124.8 (NH*Ar*$NH_2$), 113.7 (NH*Ar*$NH_2$). $^{19}$F NMR ($CDCl_3$, 471 MHz): δ -96.3 (2F, NC*F*CFC), -157.8 (2F, NCFC*F*C). Anal Calcd for $C_{11}H_7F_4N_3$ (257.06): C, 51.37; H, 2.74; N, 16.34; Found: C, 51.31; H, 2.76; N, 16.55.

*$N^1$-(perfluoropyridin-4-yl)benzene-1,2-diamine (**13**).* Compound **13** was synthesized according to the same procedure as **2** utilizing 1,2-phenylenediamine (2.17 g, 20.0 mmol) dissolved in THF (2 mL). The product was collected as off-white crystals after 1 hr (2.02 g, 86%). Crystalline product collected by this method was of sufficient quality for single-crystal x-ray diffraction. The isolated solid lacks solubility in common organic solvents, preventing further spectroscopic characterization. Mp 160 °C. Anal Calcd for $C_{11}H_7F_4N_3$ (257.06): C, 51.37; H, 2.74; N, 16.34; Found: C, 51.20; H, 2.75; N, 16.54.

*2-((perfluoropyridin-4-yl)amino)ethan-1-ol (**14**).* A 250 mL round-bottom flask was charged with DMF (57 mL), triethylamine (4.66 mL, 33.6 mL), aminoethanol (2.03 mL, 33.6 mmol), and perfluoropyridine (3.69 mL, 33.6 mmol and allowed to stir at room temperature for 36 hours. The resulting solution was extracted with diethylether (3 x 50 mL), then the combined ether fractions were washed with brine (3 x 50 mL) and dried over MgSO4. Removal of solvent in vacuo afforded target compound as a white solid (4.99 g, 70%). Crystals suitable for single-crystal X-ray diffraction were obtained by the slow evaporation of a benzene solution. Mp 82 °C. $^1$H NMR (acetone-$d_6$, 500 MHz): δ 6.24 (1H, *s*), 4.22 (1H, *s*), 3.75 (2H, *d*, $^3J_{HH}$ = 4.5 Hz), 3.62 (2H, *q*, $^3J_{HH}$ = 6.0 Hz).

$^{13}C\{^{1}H\}$ NMR ($CDCl_3$, 126 MHz): δ 145.5–143.3 (*m*), 138.0-137.6 (*m*), 132.6–130.4 (*m*), 61.7, 46.5. $^{19}F$ NMR ($CDCl_3$, 471 MHz): δ -94.0 (2F, NC*F*CFC), -163.7 (2F, NCFC*F*C). Anal Calcd for $C_7H_6F_4N_2O$ (210.04): C, 40.01; H, 2.88; N, 13.33; Found: C, 39.81; H, 2.93; N, 13.42.

*1,1'-((perfluoropyridin-4-yl)azanediyl)bis(propan-2-ol) (**15**).* Compound **15** was synthesized according to the same procedure as **2** utilizing diisopropanolamine (2.67 g, 20.0 mmol). The product was collected as off-white crystals after 7 days (1.73 g, 67%). Crystalline product collected by this method was of sufficient quality for single-crystal x-ray diffraction. Mp 122 °C. $^{1}H$ NMR (acetone-$d_6$, 500 MHz): δ 4.08–3.97 (4H, *m*, $NCH_2CH(CH_3)OH$ & $NCH_2CH(CH_3)OH$), 3.76–3.34 (4H, *m*, $NCH_2CH(CH_3)OH$), 1.12 (6H, *d*, $^{3}J_{HH}$ = 6 Hz, $NCH_2CH(CH_3)OH$). $^{13}C\{^{1}H\}$ NMR (acetone-$d_6$, 126 MHz): δ 146.8–144.4 (*m*), 141.9–141.6 (*m*), 137.8–135.3 (*m*), 64.5 ($NCH_2CH(CH_3)OH$), 61.2 (*t*, $J_{CF}$ = 4.8 Hz, $NCH_2CH(CH_3)OH$), 21.2 ($NCH_2CH(CH_3)OH$). $^{19}F$ NMR ($CDCl_3$, 471 MHz): δ -96.9 (2F, NC*F*CFC), -153.0 (2F, NCFC*F*C). Anal Calcd for $C_{11}H_{14}F_4N_2O_2$ (282.10): C, 46.81; H, 5.00; N, 9.93; Found: C, 46.50; H, 5.01; N, 9.94.

*4-(perfluoropyridin-4-yl)morpholine (**16**).* Compound **16** was synthesized according to the same procedure as **2** utilizing morpholine (1.57 mL, 20.0 mmol). The product was collected as colorless crystals after 7 days (1.87 g, 87%). Crystalline product collected by this method was of sufficient quality for single-crystal x-ray diffraction. Mp 52 °C. $^{1}$H NMR (acetone-$d_6$, 500 MHz): δ 3.78 (4H, *t*, $^{3}J_{HH}$ = 3.5 Hz), 3.53 (4H, *br s*). $^{13}$C{$^{1}$H} NMR ($CDCl_3$, 126 MHz): δ 146.7–144.3 (*m*), 141.4–140.9 (*m*), 137.3–134.8 (*m*), 67.5 ($NCH_2CH_2O$), 51.3 (*t*, $^{4}J_{CF}$ = 4.9 Hz, $NCH_2CH_2O$). $^{19}$F NMR ($CDCl_3$, 471 MHz): δ -96.0 (2F, NC*F*CFC), -155.5 (2F, NCFC*F*C). Anal Calcd for $C_9H_8F_4N_2O$ (236.06): C, 45.77; H, 3.41; N, 11.86; Found: C, 45.68; H, 3.46; N, 12.12.

*3,5-dimethyl-1-(perfluoropyridin-4-yl)piperazine (**17**).* Compound **17** was synthesized according to the same procedure as **2** utilizing 2,6-dimethylpiperazine (2.29 g, 20.0 mmol) dissolved in EtOH (7 mL). The product was collected as colorless crystals after 7 days (1.96 g, 82%). Crystalline product collected by this method was of sufficient quality for single-crystal x-ray diffraction. Mp 38 °C. $^{1}$H NMR ($CDCl_3$, 500 MHz): δ 3.52–3.44 (2H, *m*, $NHCH(CH_3)CH_2$), 3.02–2.74 (4H, *m*, $NHCH(CH_3)CH_2$), 1.46 (1H, *br s*, $NHCH(CH_3)CH_2$), 1.05 (6H, *s*, $NHCH(CH_3)CH_2$). $^{13}$C{$^{1}$H} NMR ($CDCl_3$, 126 MHz): δ

146.1–143.8 (*m*), 140.2–139.8 (*m*), 136.1–133.3 (*m*), 56.8, 51.2, 19.3. $^{19}$F NMR ($CDCl_3$, 471 MHz): δ -93.4 (2F, NC*F*CFC), -154.4 (2F, NCFC*F*C). Anal Calcd for $C_{11}H_{13}F_4N_3$ (263.10): C, 50.19; H, 4.98; N, 15.96; Found: C, 49.90; H, 5.05; N, 16.29.

**Perfluoropyridine cocrystal synthesis.** *Dicyclohexylamine•perfluoropyridine cocrystal (**18**).* Cocrystal **18** was synthesized according to the same procedure as **2** utilizing dicyclohexylamine (1.81 mL, 9.11 mmol), resulting in cocrystal formation. The product was collected as colorless crystals after 48 hrs (2.19 g, 87%). Crystalline product collected by this method was of sufficient quality for single-crystal x-ray diffraction. $T_{decomp}$ 190 °C. Phase purity was confirmed by powder x-ray diffraction. Anal Calcd for $C_{17}H_{23}F_5N_2$ (350.18): C, 58.28; H, 6.62; N, 8.00; Found: C, 58.02; H, 6.71; N, 8.09.

*2-methylpiperdine•perfluoropyridine co-crystal (**19**).* Cocrystal **19** was synthesized according to the same procedure as **2** utilizing 2-methylpiperadine (1.07 mL, 9.11 mmol) in acetonitrile, resulting in co-crystal formation. The product was collected as colorless crystals after 7 days (1.74 g, 71%). Crystalline product collected by this method was of sufficient quality for single-crystal x-ray diffraction. Mp 180 °C. Phase purity was

confirmed by powder x-ray diffraction. Anal Calcd for $C_{11}H_{13}F_5N_2$ (268.10): C, 49.26; H, 4.89; N, 10.44; Found: C, 49.12; H, 4.98; N, 10.65.

## RESULTS AND DISCUSSION

**Synthesis of 4-amino-2,3,5,6-tetrafluoropyridines.** Addition of protic, unhindered amines *para* to the pyridine nitrogen of **1** was first accomplished using a molar equivalent of reactive amine combined in absolute ethanol (Figure 1). A second equivalent of amine acts as the base in this system. The reaction was conducted at 0°C for two reasons: (1) to prevent boil-off of solvent and/or reactants from the exothermic reaction and to (2) facilitate precipitation of the products. A white solid was obtained in as little as 5 mins, which could be filtered, washed with additional ethanol, and vacuum dried to yield products **2**–**17** in good to excellent isolated yields. The amine-HF salt formed from the reaction remained soluble in all cases and was therefore easily removed from the target product. In the case of **10**–**12** and **14**–**16**, the material obtained directly from the reaction mixture was of sufficiently high crystallinity to facilitate single-crystal X-ray analysis. The operational simplicity of this methodology is evidenced by the lack of a separate base that was necessary in previously reported methods, which

allows for direct isolation of the product from the reaction mixture, without the need for additional liquid-liquid extraction steps or chromatographic work-up.

Importantly, this set of conditions afforded access to products starting from a wide range of amines. Ethanediamine, propanediamine, and hexanediamine afforded the disubstituted products **2**–**4** respectively. With these primary amines, only one substitution occurs at each amine, leaving the second hydrogen atom available for hydrogen bond donation. It is presumed the addition does not proceed further due to the steric requirements of a second perfluoropyridine on the nitrogen. When utilizing diethylenetriamine, product **5** is obtained, again resulting from the single addition to each primary amine. This product is insoluble in ethanol and precipitates nearly immediately upon formation. In an effort to further substitute this amine, diethylenetriamine was combined with six equivalents of perfluoropyridine and heated to reflux. Upon cooling, the $^{19}$F NMR revealed some degree of higher order substitution had occurred. Compound **6** has been previously prepared by Ranjbar-Karimi et. al., but starting from **5**. By the present method, conditions could not be determined to provide cleanly a single product starting directly from the unsubstituted amine; however, a small

crystalline sample of **6** was obtained from the crude reaction mixture and was suitable for crystallographic analysis. Further selectivity is observed for **11**–**14**. When starting from *para*- and *ortho*-phenylenediamine, addition occurs only to one amine, leaving the other primary amine intact. This selectivity is confirmed by both $^{1}$H NMR and the single-crystal X-ray diffraction analysis. When utilizing the aminoalcohols 2-aminoethanol and diisopropanolamine, products **14** and **15** are formed respectively. These additions are chemoselective to the amine, leaving the alcohol functionality intact. Unfortunately, **14** was not observed to react without the presence of an additional base. A compound bearing multiple types of traditional hydrogen bond donors being important to the crystallographic study, triethylamine was used to facilitate this addition. Finally, 2,6-dimethylpiperazine was chosen to probe the influence of the steric environment around the amine on the extent of the addition. In the resulting product **17**, addition is observed only to the unhindered nitrogen. This is presumably due to the steric influence of the neighboring methyl groups on the remaining amine. Addition of excess perfluoropyridine to the reaction mixture does not force the reaction to occur at this site.

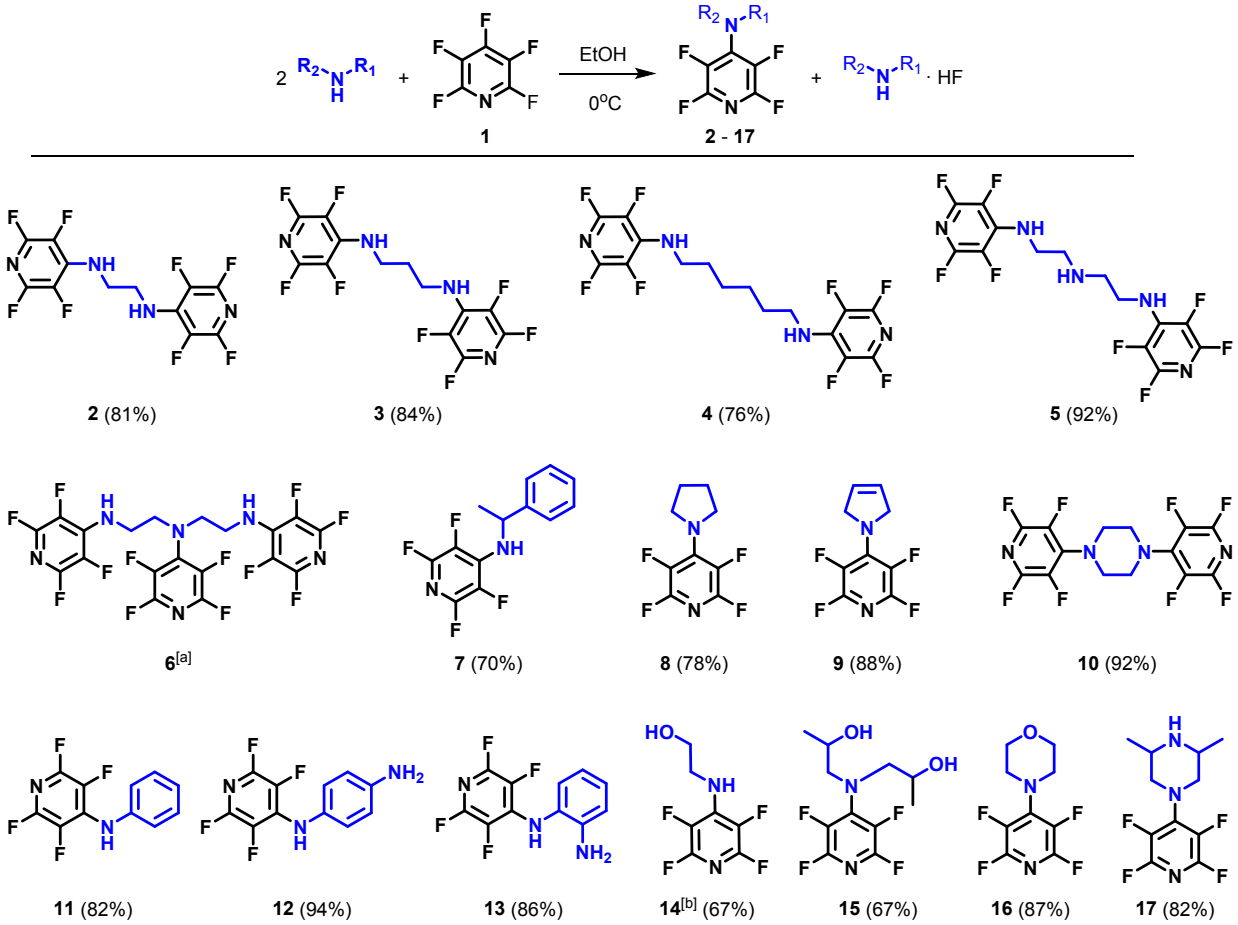


**Figure 1.** Scope of amine additions. Unless otherwise specified, the reaction was carried out on a 0.9 mmol scale with respect to perfluoropyridine in EtOH at 0°C with 2 molar equiv. of amine. [a] Crystal of **6** isolated from crude reaction mixture resulting from diethylenetriamine (0.9 mmol) and perfluoropyridine (5.4 mmol). [b] Reaction conditions: aminoethanol (33.6 mmol), perfluoropyridine (33.6 mmol), triethylamine (33.6 mmol), DMF (57 mL) at room temperature for 36 hrs.

**Hydrogen Bonding in 4-amino-2,3,5,6-tetrafluoropyridines.** The diverse nature of this pool of 4-amino-tetrafluoropyridines allowed for the study of the role of *X*–H•••F–C hydrogen bonding in crystal packing with traditional hydrogen bond acceptors such as nitrogen and oxygen, as well as in the absence any traditional acceptors. All compounds accessed by this method were studied via single-crystal X-ray diffraction, except for **7** which is a liquid under ambient conditions (See SI). For consistency with previous studies, all H atoms were moved along their valence-bond directions to make the bond lengths equal to average neutron-diffraction values.[33,34] Compounds **2**–**6**, resulting from aliphatic polyamines, each have a dominant N–H•••N intermolecular interaction involving the pyridine nitrogen, ranging in H•••N distance from 2.246(17) Å in **5** to 2.31(3) Å in **6**. This occurs despite the electron deficient nature of this nitrogen atom due to the fluorination on the ring. The secondary amines serve only as hydrogen bond donors in each structure. Of note in this series is **3**, where a variety of intermolecular interactions with fluorine are also observed (Figure 2). The C6–H•••F5(a)–C contact occurs at 2.415 Å and 144.76°, which is incidental to the N2–H•••N4(a) hydrogen bond, involving the C–F *ortho* to the pyridine nitrogen atom and a

C–H *alpha* to the amine. Also incidental to the N2–H•••N4(a) hydrogen bond is the C–F6•••F8(a)–C interaction between the other *ortho* C–F of the pyridine ring and *meta* C–F of a second ring. This fluorine-fluorine interaction occurs well below the sum of the van der Waals radii, at a F•••F distance of 2.655(3) Å and C–F•••F angles of 160.20(16)° and 125.31(18)°.[35] Additionally, two crystalline polymorphs of **2** were identified (see Figures SI29–SI33). The major difference in the structure of the two polymorphs is the plane-to-plane angle between pyridine rings on each end of the ethanediamine linker, from 57.18(5)° to 22.22(9)°. As in **3**, the intermolecular interactions are dominated by N–H•••$N_{pyridine}$ contacts in both polymorphs of **2**, at H•••N distances of 2.17(2) Å and 2.28(2) Å. The primary C–H•••F–C contact is shorter (2.412 Å) when the plane-to-plane angle is decreased, as the contact is incidental to the N–H•••N hydrogen bond.

Of the compounds derived from aromatic amines, **11** shows the shortest such N–H•••N interaction at 2.04(3) Å. The longest of the series is in **13**, at H•••N1 distance of 2.423(19) Å. Compound **12**, for which the structure has been previously reported by Ranjibar and co-workers is intermediate, at 2.27(2) Å.[32] In **14**, a O–H•••N hydrogen bond with the pyridine nitrogen at 1.934(18) Å and 155.8(16)° allows for the formation of

crystallographic dimers. In **15**, the packing forces are dominated by O–H•••O hydrogen bonds and no significant interactions with the pyridine nitrogen are observed.

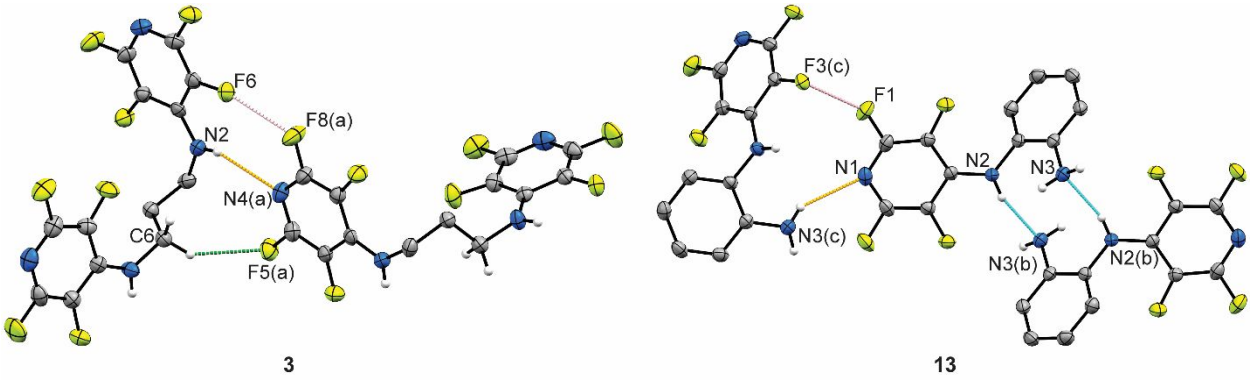


**Figure 2.** Solid state structures of **3** and **13** exhibiting characteristic intermolecular interactions in compound **2**–**6** and **8**–**17**. Intermolecular Npyridine•••H–N (orange), Namine•••H–N (teal), F•••H–C (green), and C–F•••F–C (pink) interactions are indicated by dashed lines. H atoms, except those bound to the donor atoms of the indicated intermolecular interactions, have been omitted for clarity. Thermal ellipsoids are shown at the 50% probability level. Symmetry generated atoms are generated by the following operations: (a) 1 + *x*, 1 + *x* – *y*, 1 – *z*; (b) 1 – *x*, –*y*, 1 – *z*; (c) 0.5 – *x*, 0.5 + *y*, 0.5 – *z*.

**N–H•••F–C Hydrogen Bonding Cocrystals with Perfluoropyridine.** Finally, the combination of **1** and hindered amines such as dicyclohexylamine and 2-

methylpiperdine resulted in the formation of cocrystals **18** and **19** respectively (Figure 3). In **18**, the *para* C–F bond of perfluoropyridine participates in a strong hydrogen bonding interaction with the dicyclohexylamine N–H, with a H•••F3 distance of 1.95(5) Å and a N2–H•••F3 angle of 169(5)°. Furthermore, C–H•••F–C close contacts also occur for the remaining two C–F bonds, at a distance of 2.282 Å and angle of 132° for the *meta* C–F2 and 2.521 Å and 122° for the *ortho* C–F. Surprisingly, it is the pyridine nitrogen which has the longest hydrogen bonding interaction, occurring at a H•••N1 distance of 2.670 Å and angle of 127° to a cyclohexyl ring in the next layer of cyclohexyl amines (see Figure SI41). While the 2- and 6- position fluorine atoms of **1** may induce some steric encumbrance around the pyridine nitrogen, three cocrystals involving hydrogen bonding between the nitrogen atom of 2,6-dicarboxypyridine derivatives and the ammonium hydrogen atoms dicyclohexylammonium cations have been previously reported, with N–H•••N contact distances ranging from 2.260(2) Å to 2.588 Å.[36–38] These contacts are incidental to much shorter N–H•••O contacts to the carboxy moiety.

The packing in **19** follows a similar pattern to **18**. A N–H•••F–C hydrogen bond is still the primary intermolecular interaction. Due to the

expected disorder arising from the ring inversion of the 6-membered piperdine ring, two piperdine ring positions can be refined in the crystallographic data. Considering only the primary component, the N2(a)–H•••F3–C contact occurs at an H•••N distance of 1.757(19) Å and an angle 165(5)°. In contrast to **18**, only the *meta* C–F2 is involved in C–H•••F–C hydrogen bonding in **19**; however, there are four distinct interactions of this type: 2.572 Å and 140°; 2.395 Å and 145°; 2.455 Å and 132°; 2.607 Å and 128°. Again, it is the pyridine nitrogen which shows the longest hydrogen bonding interaction to a neighboring piperdine ring, occurring at a H•••N1 distance of 2.663 Å and an angle of 121° to a C–H bond of the primary disorder component (see Figure SI42). The unexpected nature of the N–H•••F–C contact in both **18** and **19** is qualitatively reinforced when the molecular electrostatic potential is mapped on the Hirshfeld surface, as the *para* fluorine of perfluoropyridine contributes to the most electropositive portion of the surface. Additionally, perfluoropyridine rings pack parallel to each other, with a ring plane-to-ring plane distance of 3.523(3) Å. This π-π interaction is not seen in the previously reported solid-state structure of **1**.[39,40] This cocrystal also reveals a potential shortcoming in many of the previous studies involving database surveys,

namely the exclusion of disordered structures. If that constraint were applied to this compound, it would have been excluded, despite a chemically valid reason (6-membered ring inversion) for the disorder.

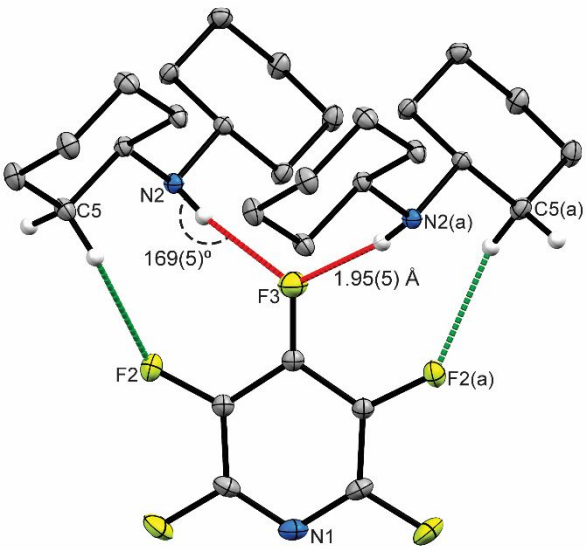


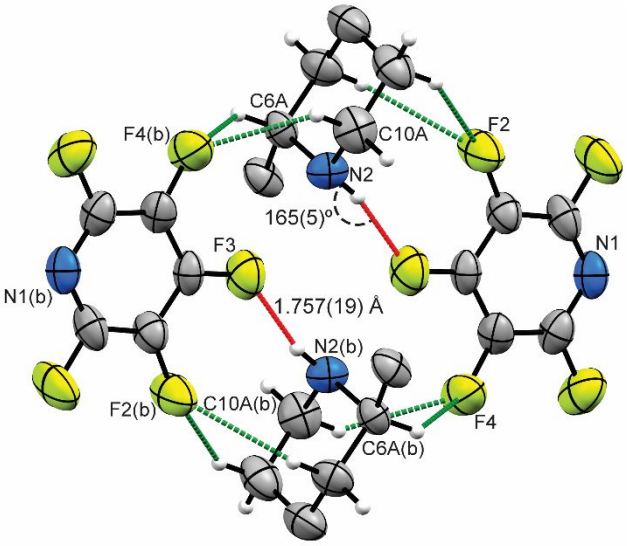


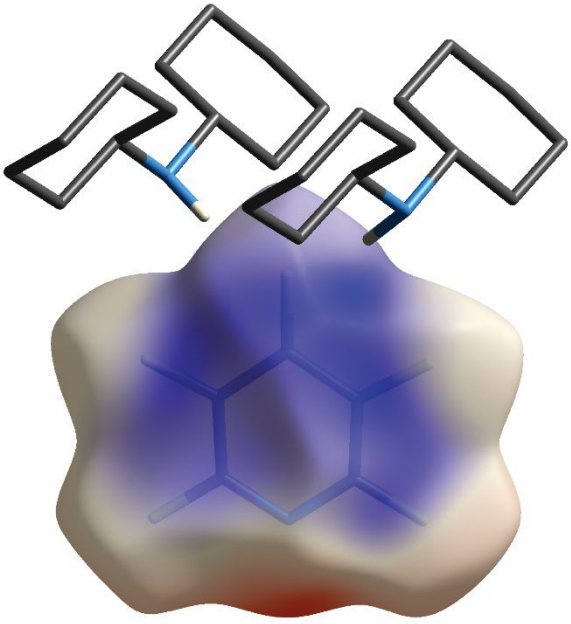

18

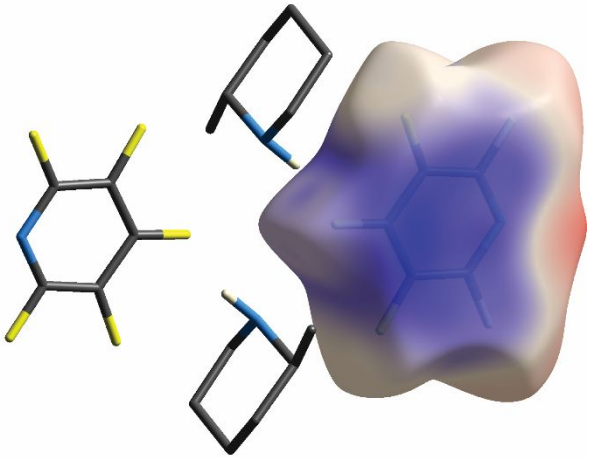

19

**Figure 3.** Solid state structures (top) and the molecular electrostatic potential mapped on the Hirshfeld surface (bottom) of **18** and **19**. Intermolecular F•••H–N (red) and F•••H–C (green) interactions are indicated by dashed lines. H atoms, except those bound to the donor atoms of the indicated intermolecular interactions, have been omitted for clarity. Thermal ellipsoids are shown at the 50% probability level. Symmetry generated atoms are generated by the following operations: (a) 2 – *x*, *y*, 0.5 – *z*; (b) 1.5 – *x*, 0.5 – *y*, 1 – *z*.

Based on a survey of the CSD, the N–H•••F–C interaction in **19** is the shortest such hydrogen bond involving a neutral amine reported to date. While still correcting H atom distances to the neutron distance, the next closest N–H•••F–C reported with a neutral amine involves a C–F bond of a cyclopropane ring acting at a H•••N distance of 2.083(4) Å, approximately 0.2 Å longer than that in **19** (Figure 4a).[41] The only shorter N–H•••F–C interaction in the CSD occurs at a slightly shorter H•••N distance of 1.646(2) Å, between the ammonium N–H of tetramethylethylenediammonium and the carbanion C–F in difluoro(pentafluorophenyl)methanide (Figure 4b).[42] In this case, the formal

charge state of both the ammonium and carbanion are activating towards strong hydrogen bonds.

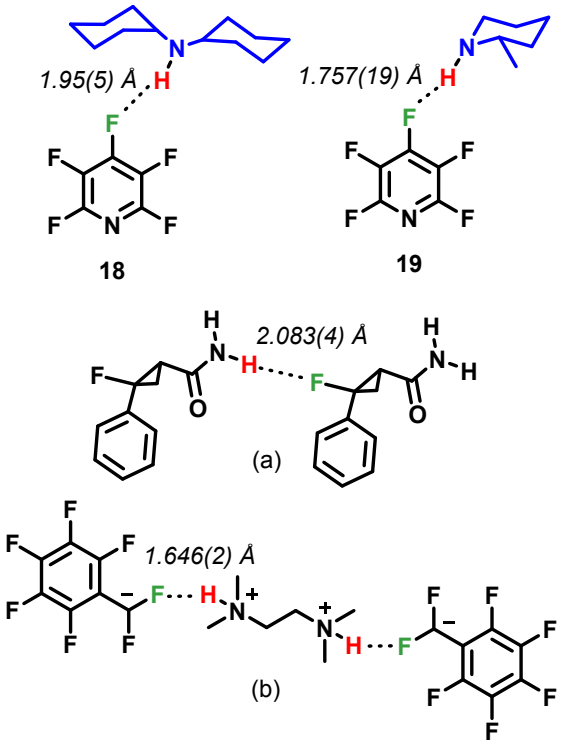


**Figure 4.** Cocrystals **18** and **19**. (a) *cis*-2-fluorophenylcyclopropylcarboxyamide. (b) *N*,*N*,*N*′,*N*′-tetramethylethylene-diammonium bis(difluoro(pentafluorophenyl)methanide)

The strong intermolecular interactions within cocrystals **18** and **19** impart significant thermal stability, as indicated by a simultaneous differential scanning calorimetry–thermogravimetric analysis (Figure 5). In **18**, the onset of decomposition is observed at approximately 190 °C, far above the boiling point of pentafluoropyridine (83 °C).

Decomposition concludes at approximately 230 °C, with a 12% char yield. An endotherm corresponding to the vaporization of unreacted dicyclohexylamine is observed at 264 °C. No concomitant mass loss is observed, indicative of only trace amounts. In **19**, onset of mass loss occurs at approximately 180 °C, well above the boiling points of pentafluoropyridine and 2-methylpiperidine (118 °C). Mass loss concludes at 223 °C, in this case with no char yield. In both cases, the cocrystals seem to be indefinitely stable at ambient conditions.

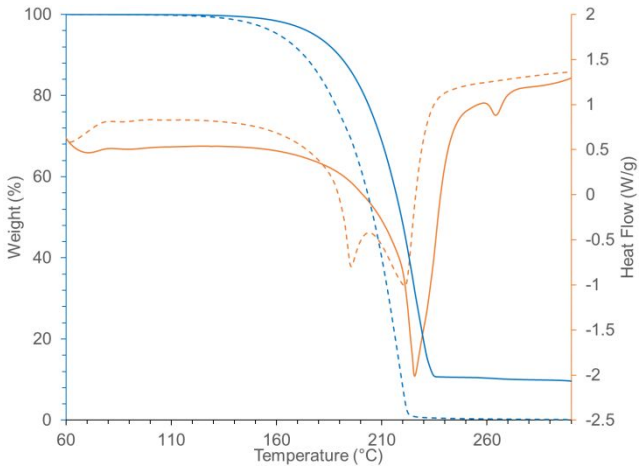


**Figure 5.** Combined DSC (orange) and TGA (blue) for **18** (solid) and **19** (dashed).

Comparison of the type, distance, and number of hydrogen bonding contacts provides further context to the high melting points of **18** and **19** (Table 1). Formed from linear diamines, **2**–**5** all show hydrogen bonding interactions involving the pyridine nitrogen

and the amine N–H, and the melting points are similar to one another, between 114 °C (**4**) and 125 °C (**3**). Products **8**, **9**, and **16** are unremarkable in terms of hydrogen bonding; however, the planarity of pyrroline versus pyrrolidine and morpholine allows for significant π–π interactions, raising the melting point from 49 °C in **8** and 71 °C in **16**, to 122 °C in **9**. Compound **10** has a melting point only 10 °C higher than cocrystal **18**. Its previously reported solid-state structure shows no traditional hydrogen bonding interactions, though C–H•••F interactions are present.[31] Its thermal stability can be attributed a series of C–F•••π interactions.

**Table 1.** *X*–H••• *Y* interactions within the sum of the van der Waals radii in the crystal structures of **2**–**19**.

| Product | Contact type | Closest distance (Å) | No. of contacts | Melting point (°C) |
|---|---|---|---|---|
| **2**[a] | N–H···$N_{pyridine}$<br>C–H···F | 2.23(4)<br>2.534 | 2<br>2 | 115 |
| **3** | N–H···$N_{pyridine}$<br>C–H···F | 2.28(3)<br>2.415 | 2<br>5 | 125 |
| **4** | N–H···$N_{pyridine}$<br>C–H···F | 2.264(17)<br>2.610 | 2<br>4 | 114 |
| **5** | N–H···$N_{pyridine}$<br>N–H···$N_{amine}$<br>C–H···F | 2.246(17)<br>1.963(18)<br>2.350 | 2<br>1<br>4 | 115 |
| **8**[b] | C–H···$N_{pyridine}$<br>C–H···F | 2.625<br>2.533 | 1<br>4 | 49 |
| **9** | C–H···$N_{pyridine}$<br>C–H···F | 2.561<br>2.470 | 1<br>3 | 122 |
| **10**[c] | C–H···F | 2.455 | 2 | 200 |

| | | | | |
|---|---|---|---|---|
| **11** | N–H···$N_{Pyr}$ | 2.04(3) | 1 | 96 |
| | C–H···F | 2.425 | 3 | |
| **12**[d] | N–H···$N_{pyridine}$ | 2.27(2) | 1 | 191 |
| | N–H···$N_{amine}$ | 2.188(17) | 1 | |
| | C–H···F | 2.327 | 2 | |
| **13** | N–H···$N_{pyridine}$ | 2.423(19) | 1 | 160 |
| | N–H···$N_{amine}$ | 2.020(19) | 1 | |
| | C–H···F | 2.441 | 4 | |
| **14** | N–H···O | 1.869(17) | 1 | 82 |
| | O–H···$N_{pyridine}$ | 1.934(18) | 1 | |
| | C–H···F | 2.430 | 4 | |
| **15**[b] | O–H···O | 1.813(17) | 2 | 122 |
| | C–H···F | 2.428 | 5 | |
| **16**[b] | C–H···$N_{pyridine}$ | 2.656 | 1 | 71 |
| | C–H···F | 2.496 | 3 | |
| **18** | N–H···F | 1.95(5) | 1 | 190 |
| | C–H···$N_{pyridine}$ | 2.670 | 2 | |
| | C–H···F | 2.282 | 6 | |
| **19**[b] | N–H···F | 1.757(19) | 1 | 180 |
| | C–H···$N_{pyridine}$ | 2.663 | 1 | |
| | C–H···F | 2.398 | 5 | |

Pure, single-crystal X-ray diffraction quality material of **17** could not be obtained. In an effort to force cocrystal formation of **17** with **1**, it was recrystallized from neat **1**, revealing the dihydrate of **17** formed with adventitious water, with no additional perfluoropyridine in the lattice (Figure 6). With a methyl group *alpha* to both sides of the secondary amine, a hydrogen bonding interaction with **1** is discouraged. This result emphasizes the influence of the steric environment on this hydrogen bonding interaction.

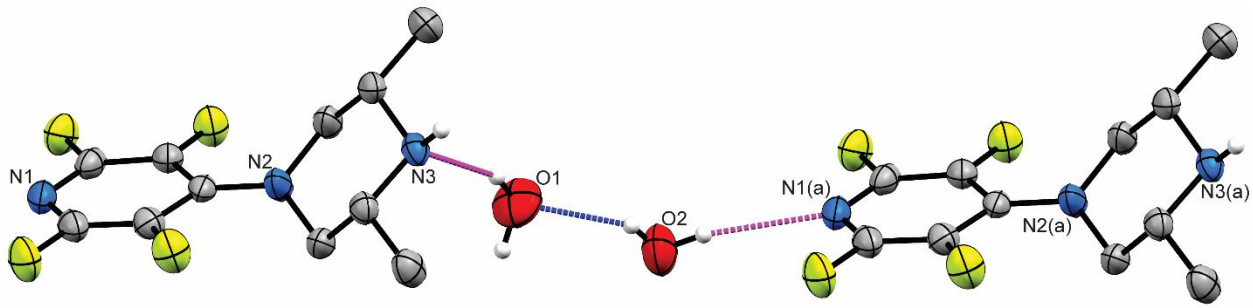


**Figure 6.** Solid state structure of **17•2H$_2$O**. Intermolecular N•••H–O (magenta) and O•••H–O (blue) interactions are indicated by dashed lines. H atoms, except those bound to the donor atoms of the indicated intermolecular interactions, have been omitted for clarity. Thermal ellipsoids are shown at the 50% probability level. Symmetry generated atoms are generated by the operation (a) – 1 + *x*, *y*, *z*.

To the authors' knowledge, only one solid cocrystal system comprised of nonreacting liquids has been previously reported; however, this system consisted of oligomeric polyoxacyclobutane (POCB) and water.[43] Standing in stark contrast to **18** and **19**, the melting point of a cocrystal of 2480 g/mol POCB and water is 39 °C, only 19 °C above the normal melting point for the pure POCB. The lowest molecular weight POCB to exhibit cocrystal formation was 300 g/mol, still much higher than the molecular weights

of either dicyclohexylamine (181 g/mol) or 2-methylpiperdine (99 g/mol). The 300 g/mol POCB:$H_2O$ cocrystals have a melting point of 27 °C, six times less than either **18** or **19**.

## CONCLUSIONS

In summary, we have developed a simplified method of amine addition to the *para* position of perfluoropyridine, utilizing the desired amine as both the nucleophile and base. The reaction proceeds with a broad variety of amines, providing pure product in as little as five minutes. While this study does support the overall assertion of *X*–H•••F–C interactions being a "donor's last resort," the unique electronic structure of perfluoropyridine provides access to unique interactions. In particular, an X-ray crystallographic study of solid cocrystals of nonreacting liquids when perfluoropyridine is combined with either dicyclohexylamine or 2-methylpiperdine revealed that N–H•••F–C interactions can not only be preferred over potential N–H•••N interactions, but can impart significant thermal stability. Both cocrystals are thermally stable until at least 180°C. Currently, we are focusing on additional studies to further the scope of the rare *X*–H•••F–C interaction involving perfluoropyridine.

## ASSOCIATED CONTENT

**Supporting Information**. The following files are available free of charge.

$^{1}$H, $^{13}$C{$^{1}$H}, and $^{19}$F NMR spectra of the compounds, powder x-ray diffraction patterns for **18** and **19**, crystallographic data and structure refinement parameters, and hydrogen-bond geometry data (PDF)

### Accession Codes

CCDC 1906424, 1912058, 1986043, 1994733–1994745 contain the supplementary crystallographic data for this paper. These data can be obtained free of charge via www.ccdc.cam.ac.uk/data_request/cif, or by emailing data_requests@ccdc.cam.ac.uk, or by contacting The Cambridge Crystallograhic Data Centre, 12 Union Road, Cambridge CB2 1EZ, UK; fax +44 1223 336033.

## AUTHOR INFORMATION

### Corresponding Authors

Scott T. Iacono: e-mail, scott.iacono@afacademy.af.mil

William T. Pennington: e-mail, billp@clemson.edu

## ORCID

Andrew J. Peloquin: 0000-0002-7535-2049

Abby R. Jennings: 0000-0002-4922-5759

Colin D. McMillen: 0000-0002-7773-8797

Scott T. Iacono: 0000-0002-2313-2618

William T. Pennington: 0000-0001-5224-7046

## Notes

The authors declare no competing financial interest.

## ACKNOWLEDGMENT

S.T.I. acknowledges financial support from the Air Force Office of Scientific Research (AFOSR).

## REFERENCES

(1) Monat, J. E.; Toczyłowski, R. R.; Cybulski, S. M. Ab Initio Study of the CH 3 F···H 2 O Complex † . *J. Phys. Chem. A* **2001**, *105*, 9004–9013. https://doi.org/10.1021/jp011279o.

(2) Bettinger, H. F. How Good Is Fluorine as a Hydrogen-Bond Acceptor in Fluorinated Single-Walled Carbon Nanotubes? *ChemPhysChem* **2005**, *6*, 1169–1174. https://doi.org/10.1002/cphc.200400324.

(3) Schneider, H. J. Hydrogen Bonds with Fluorine. Studies in Solution, in Gas Phase and by Computations, Conflicting Conclusions from Crystallographic Analyses. *Chem. Sci.* **2012**, *3*, 1381–1394. https://doi.org/10.1039/c2sc00764a.

(4) Mishra, S. K.; Suryaprakash, N. Organic Fluorine Involved Intramolecular Hydrogen Bonds in the Derivatives of Imides: NMR Evidence Corroborated by DFT Based Theoretical Calculations. *RSC Adv.* **2015**, *5*, 86013–86022. https://doi.org/10.1039/c5ra19537c.

(5) Biswas, B.; Singh, P. C. The Role of Fluorocarbon Group in the Hydrogen Bond Network, Photophysical and Solvation Dynamics of Fluorinated Molecules. *J.*

*Fluor. Chem.* **2019**, No. October, 109414. https://doi.org/10.1016/j.jfluchem.2019.109414.

(6) Groom, C. R.; Bruno, I. J.; Lightfoot, M. P.; Ward, S. C. The Cambridge Structural Database. *Acta Crystallogr. Sect. B Struct. Sci. Cryst. Eng. Mater.* **2016**, *72*, 171–179. https://doi.org/10.1107/S2052520616003954.

(7) Howard, J. A. K.; Hoy, V. J.; O'Hagan, D.; Smith, G. T. How Good Is Fluorine as a Hydrogen Bond Acceptor? *Tetrahedron* **1996**, *52*, 12613–12622. https://doi.org/10.1016/0040-4020(96)00749-1.

(8) Dunitz, J. D.; Taylor, R. Organic Fluorine Hardly Ever Accepts Hydrogen Bonds That the Jattep Can Be Expected to Hydrogen-Bond to Water Or. *Chem. Eur. J.* **1997**, *3*, 89–98.

(9) Brammer, L.; Bruton, E. A.; Sherwood, P. Understanding the Behavior of Halogens as Hydrogen Bond Acceptors. *Cryst. Growth Des.* **2001**, *1*, 277–290. https://doi.org/10.1021/cg015522k.

(10) Shimoni, L.; Glusker, J. P. The Geometry of Intermolecular Interactions in Some Crystalline Fluorine-Containing Organic Compounds. *Struct. Chem.* **1994**, *5*, 382–397.

(11) Chopra, D. Is Organic Fluorine Really "Not" Polarizable? *Cryst. Growth Des.* **2012**, *12*, 541–546. https://doi.org/10.1021/cg201498u.

(12) Thalladi, V. R.; Weiss, H. C.; Bläser, D.; Boese, R.; Nangia, A.; Desiraju, G. R. C-H···F Interactions in the Crystal Structures of Some Fluorobenzenes. *J. Am. Chem. Soc.* **1998**, *120*, 8702–8710. https://doi.org/10.1021/ja981198e.

(13) Berger, R.; Resnati, G.; Metrangolo, P.; Weber, E.; Hulliger, J. Organic Fluorine Compounds: A Great Opportunity for Enhanced Materials Properties. *Chem. Soc. Rev.* **2011**, *40*, 3496–3508. https://doi.org/10.1039/c0cs00221f.

(14) Reichenbächer, K.; Süss, H. I.; Hulliger, J. Fluorine in Crystal Engineering - "The Little Atom That Could." *Chem. Soc. Rev.* **2005**, *34*, 22–30. https://doi.org/10.1039/b406892k.

(15) Taylor, R. The Hydrogen Bond between N-H or O-H and Organic Fluorine: Favourable Yes, Competitive No. *Acta Crystallogr. Sect. B Struct. Sci. Cryst. Eng. Mater.* **2017**, *73*, 474–488. https://doi.org/10.1107/S2052520617005923.

(16) Fuhrer, T. J.; Houck, M.; Corley, C. A.; Iacono, S. T. Theoretical Explanation of Reaction Site Selectivity in the Addition of a Phenoxy Group to Perfluoropyridine. *J. Phys. Chem. A* **2019**, *123*, 9450–9455. https://doi.org/10.1021/acs.jpca.9b06413.

(17) Beyki, K.; Haydari, R.; Maghsoodlou, M. T. Synthesis of 2,3,5,6-Tetrafluoro-Pyridine Derivatives from Reaction of Pentafluoropyridine with Malononitrile, Piperazine and Tetrazole-5-Thiol. *Springerplus* **2015**, *4*, 1–7. https://doi.org/10.1186/s40064-015-1495-4.

(18) Beverina, L.; Drees, M.; Facchetti, A.; Salamone, M.; Ruffo, R.; Pagani, G. A. Bulk Heterojunction Solar Cells-Tuning of the HOMO and LUMO Energy Levels of Pyrrolic Squaraine Dyes. *European J. Org. Chem.* **2011**, No. 28, 5555–5563. https://doi.org/10.1002/ejoc.201100940.

(19) Litvak, V. V.; Mainagashev, I. Y.; Bukhanets, O. G. Chemistry and Dynamics of Interaction of Nucleosides with Pentafluoropyridine. *Nucleosides, Nucleotides and Nucleic Acids* **2005**, *24*, 1373–1385. https://doi.org/10.1080/15257770500230772.

(20) Beletskaya, I. P.; Artamkina, G. A.; Ivushkin, V. A.; Guilard, R. Arylation of Polyamines by Perfluoroarenes. *Tetrahedron Lett.* **2000**, *41*, 313–316. https://doi.org/10.1016/S0040-4039(99)02081-X.

(21) Laot, Y.; Petit, L.; Zard, S. Z. Synthesis of Fluoroazaindolines by an Uncommon Radical Ipso Substitution of a Carbon-Fluorine Bond. *Org. Lett.* **2010**, *12*, 3426–3429. https://doi.org/10.1021/ol101240f.

(22) West, C. W.; Adler, M.; Arnaiz, D.; Chen, D.; Chu, K.; Gualtieri, G.; Ho, E.; Huwe, C.; Light, D.; Phillips, G.; et al. Identification of Orally Bioavailable, Non-Amidine Inhibitors of Urokinase Plasminogen Activator (UPA). *Bioorganic Med. Chem. Lett.* **2009**, *19*, 5712–5715. https://doi.org/10.1016/j.bmcl.2009.08.008.

(23) Senaweera, S. M.; Weaver, J. D. Selective Perfluoro- and Polyfluoroarylation of Meldrums Acid. *J. Org. Chem.* **2014**, *79*, 10466–10476.

https://doi.org/10.1021/jo502075p.

(24) Xie, J.; Rudolph, M.; Rominger, F.; Hashmi, A. S. K. Photoredox-Controlled Mono- and Di-Multifluoroarylation of C(Sp3)−H Bonds with Aryl Fluorides. *Angew. Chemie - Int. Ed.* **2017**, *56*, 7266–7270. https://doi.org/10.1002/anie.201700135.

(25) Matsuda, N.; Hirano, K.; Satoh, T.; Miura, M. Copper-Catalyzed Direct Amination of Electron-Deficient Arenes with Hydroxylamines. *Org. Lett.* **2011**, *13*, 2860–2863. https://doi.org/10.1021/ol200855t.

(26) Gottlieb, H. E.; Kotlyar, V.; Nudelman, A. NMR Chemical Shifts of Common Laboratory Solvents as Trace Impurities In the Course of the Routine Use of NMR. *J. Org. Chem.* **1997**, *62*, 7512–7515. https://doi.org/10.1111/cge.13191.

(27) Bruker. APEX3. Bruker AXS: Madison, WI, USA 2015.

(28) Sheldrick, G. M. Crystal Structure Refinement with SHELXL. *Acta Crystallogr. Sect. C Struct. Chem.* **2015**, *71*, 3–8. https://doi.org/10.1107/S2053229614024218.

(29) Spackman, M. A.; Jayatilaka, D. Hirshfeld Surface Analysis. *CrystEngComm* **2009**, *11*, 19–32. https://doi.org/10.1039/b818330a.

(30) Spackman, M. A.; McKinnon, J. J.; Jayatilaka, D. Electrostatic Potentials Mapped on Hirshfeld Surfaces Provide Direct Insight into Intermolecular Interactions in Crystals. *CrystEngComm* **2008**, *10*, 377–388. https://doi.org/10.1039/b715494a.

(31) Ranjbar-karimi, R.; Khaje-Khezri, A. Environmental Friendly Synthesis of Bis-Perfluoropyridine and Pyrimidine in Water. *Heterocycles* **2015**, *91*, 738–746.

(32) Ranjbar-karimi, R.; Mashak-shoshtari, M.; Darehkordi, A. Ultrasonics Sonochemistry Ultrasound Promoted Facile Synthesis of Some Pentafluoropyridine Derivatives at Ambient Conditions. *Ultrason. - Sonochemistry* **2011**, *18*, 258–263. https://doi.org/10.1016/j.ultsonch.2010.05.017.

(33) Allen, F. H.; Kennard, O.; Watson, D. G.; Brammer, L.; Orpen, A. G.; Taylor, R. Tables of Bond Lengths Determined by X-Ray and Neutron Diffraction. Part 1. Bond Lengths in Organic Compounds. *J. Chem. Soc. Perkin Trans. 2* **1987**, No. 12, 1–19. https://doi.org/10.1039/P298700000S1.

(34) Taylor, R.; Kennard, O. Comparison of X-ray and Neutron Diffraction Results for the N-H ···O=C Hydrogen Bond. *Acta Crystallogr. Sect. B* **1983**, *39*, 133–138. https://doi.org/10.1107/S0108768183002116.

(35) Rowland, R. S.; Taylor, R. Intermolecular Nonbonded Contact Distances in Organic Crystal Structures: Comparison with Distances Expected from van Der Waals Radii. *J. Phys. Chem.* **1996**, *100*, 7384–7391. https://doi.org/10.1021/jp953141+.

(36) Ng, S. W. Bis(Dicyclohexylammonium) 2,6-Pyridinedicarboxylate Dihydrate. *Acta Crystallogr. Sect. C Cryst. Struct. Commun.* **1997**, *53*, 986–987. https://doi.org/10.1107/S010827019700293X.

(37) Ng, S. W. Dibutyltin Derivatives of 4-Hydroxy-2 , 6-Pyridine-. *Z. Krist.* **1998**, *213*, 421–426.

(38) Ng, Seik Weng; Kumar Dumas, V. G.; Tiekink, E. R. T. Structural Chemistry of Organotin Carboxylates: VII. Synthesis of Triorganostannate Esters of Dicarboxylic Acids. Crystal Structure of Dicyclohexylammonium 2,6-

Pyridinedicarboxylatotributylstannate. *J. Organometalic Chem.* **1991**, *403*, 111–117.

(39) Olejniczak, A.; Katrusiak, A.; Vij, A. Interpenetrated Structure and Compressibility Studies in Pressure Frozen Pentafluoropyridine Crystals at 0.3 and 1.1 GPa. *J. Fluor. Chem.* **2008**, *129*, 173–177. https://doi.org/10.1016/j.jfluchem.2007.10.005.

(40) Stammler, H. G.; Vishnevskiy, Y. V.; Sicking, C.; Mitzel, N. W. Charge Density Studies on 2,3,5,6-Tetrafluoro- and Pentafluoropyridine. *CrystEngComm* **2013**, *15*, 3536–3546. https://doi.org/10.1039/c3ce40332g.

(41) Haufe, G.; Rosen, T. C.; Meyer, O. G. J.; Fröhlich, R.; Rissanen, K. Sythesis, Reactions and Structural Features of Monofluorinated Cyclopropanecarboxylates. *J. Fluor. Chem.* **2002**, *114*, 189–198. https://doi.org/10.1016/S0022-1139(02)00040-4.

(42) Zhu, S.; Xing, C.; Xu, W.; Li, Z. Hydrogen Bonding and Halogen Bonding Co-Existing in the Reaction of Heptafluorobenzyl Iodide with N,N,N′,N′-Tetramethylethylene Diamine. *Tetrahedron Lett.* **2004**, *45*, 777–780.

https://doi.org/10.1016/j.tetlet.2003.11.100.

(43) Banerjee, J.; Koronaios, P.; Morganstein, B.; Geib, S. J.; Enick, R. M.; Keith, J. A.; Beckman, E. J.; Velankar, S. S. Liquids That Freeze When Mixed: Cocrystallization and Liquid-Liquid Equilibrium in Polyoxacyclobutane-Water Mixtures. *Macromolecules* **2018**, *51*, 3176–3183. https://doi.org/10.1021/acs.macromol.8b00239.

FOR TABLE OF CONTENTS USE ONLY

# Fluorinated Aminopyridines: Synthesis, Structure, and Rare Liquid-Liquid Cocrystal Formation Driven by Unusually Short N–H•••F–C Hydrogen Bonding

Andrew J. Peloquin, Daniel A. Kure, Abby R. Jennings, Colin D. McMillen,

Scott T. Iacono,* and William T. Pennington*

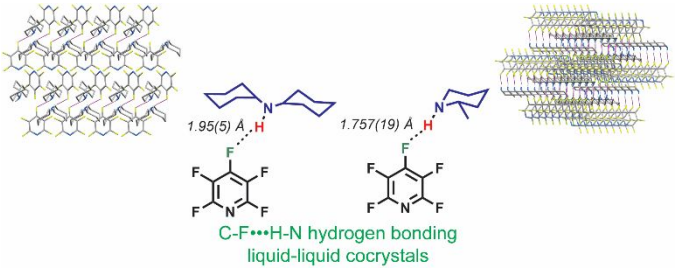


Liquid–liquid cocrystals were formed from the combination of perfluoropyridine and hindered amines. The solid state packing in these cocrystals is dominated by C–F•••H–N hydrogen bonding. When combined with unhindered primary and secondary amines, rapid substitution on the perfluoropyridine is achieved.